doi:10.1017/S1431927621003287
Microsc. Microanal. 27 (Suppl 1), 2021

Cryo-EM structure of F-actin decorated by HMM in rigor state

Alimohammad Hojjatian[1], Dianne Taylor[2], Nadia Daneshparvar[3], Patty Fagnant[4], Kathleen Trybus[5] and Kenneth Taylor[3]

[1]Florida state university, Tallahassee, Florida, United States, [2]florida state university, United States, [3]Florida State University, United States, [4]University of Vermont, United States, [5]University of Vermont College of medicine, United States

Cryo-EM 3D reconstruction has paved the way for atomic resolution structure determination of non-crystalline biological samples (*1*). For practical purposes, the presence of symmetry and homogeneity among others are extremely helpful. One type of specimen where cryoEM has made major contributions is the structure of filaments with helical symmetry, including the recent atomic resolution structures of F-actin alone (*2*) and when decorated with individual myosin heads (*3*). However, actin decorated with the double-headed myosin fragment, known as HMM, only shows helical symmetry out to approximately the end of the myosin motor domain (10 nm radius). The rest of the myosin head consists of a small, folded domain known as the "converter" and a long α-helix that binds a pair of light chains, dubbed essential (ELC), and regulatory (RLC). The lever arm amplifies small conformational changes in the myosin motor domain into a large axial movement at the end of the myosin head (*4*). The lever arms (extending a further 30 Å) cannot follow the F-actin symmetry unless the myosin coiled coil, here called the proximal S2, unfolds to accommodate the ~75 Å separation of the head-tail junctions. If the proximal S2 does not unfold, then the two lever arms must assume different structures which will impart some strain into the system and break the helical symmetry thus removing the most powerful feature of helical filaments for structure determination. Structures of myosin heads bound to actin in situ in muscle show the two lever arms coming together to a common origin rather than indicating separation due to unfolding of the proximal S2 (*5, 6*) at low resolution. The structure of F-actin decorated with HMM has only been investigated once previously using negative stain and imposition of helical symmetry (*7*). A structure of two-headed myosin II binding to F-actin is important for a mechanical description of force production in muscle. Here we use single particle reconstruction to test a protocol for avoiding imposition of helical symmetry and use frozen-hydrated specimens for improving specimen preservation and thereby assess prospects for high resolution structure determination of HMM decorated actin.

For sample preparation, chicken smooth muscle HMM was expressed similar to (*8*). F-actin was mixed with HMM in the presence of ATP on a lipid monolayer doped with a Ni-NTA lipid (*9*). After manually blotting and plunge freezing the grids, a cryo-EM dataset was collected on a Titan-Krios microscope equipped with a DE-64 direct electron detector and Volta Phase plate to amplify the phase contrast (*10*). Movies were preprocessed in cisTEM (*11*), manually picked and ~500Å long segments were extracted in Relion (*12*). Class averages of projections showed the classic arrowhead structure (Fig. 1a,b). cisTEM 3D Autorefinement resulted in a ~14Å 3D map as determined by FSC using the 0.143 criteria. While showing some detailed features within the core of the filaments including F-actin and the myosin motor domains (Fig. 1c), the density outside of the corresponding diameter was poorly defined. Application of the auto-masking feature in cisTEM proved necessary to obtain a reconstruction. After rounds of the 2D classification and selection of segments with better quality, the iterative helical real-space reconstruction algorithm implemented in Relion (*12*) was utilized for an alternative 3D refinement. The result processed by MonoRes (*13*) demonstrates spatially varying resolution (Fig. 1c). After one round of 3D classification, selection of segments from two best looking classes and 3D refinement of the selected segments, the result

was subjected to masked 3D classification encompassing one HMM unit, as shown with a transparent density in Figure 1c. Classification revealed different conformations including two-headed, shifted two-headed and one-headed decorations (Fig. 1d-g).

Result of the refinement of the combined similar classes demonstrated noticeable distinction between classes, despite the limited number of segments. The classes with single-headed decorations hinted to the development of a "parking problem" (Fig. 1d,e) when as F-actin becomes increasingly saturated with myosin heads, fewer sites are available with a pair of adjacent, unoccupied actin subunits. We built a model of the class with the best resolved lever arm pair (Fig. 1f). We combined parts of three different atomic models from different studies (PDB 6BIH, 6XE9 and 1KK7) (*14-16*) along with SWISS model (*17*) to take advantage of homology modeling combined with semi-rigid fitting of the atomic model into the density map. Small manual modifications were performed using Coot (*18*) to resolve geometrical issues.

The atomic model utilized a motor domain-actin structure (*14*) which fits very well into the density near actin (Fig. 2a). Both lever arms had to be modified after placing the light chain binding domain into the density as a rigid body. The forward head on the (-) side of the structure required a slight downward tilt of its RLC domain to fit the density. The trailing head on the (+) side of the F-actin required tilting upward of the RLC domain to fit the density (Fig. 2a,b), resulting in 21Å distance between the head-tail junctions (residues 851) of the two lever arms. Slight changes were needed in the converter and ELC segments. When the forward and trailing motor domains were superimposed the lever arms sweep out an axial distance of 72 Å measured at the head-tail junctions (Fig. 2c,d), a plausible power stroke distance. An azimuthal angle change imposed by the helical twist of actin is also observed.

Our study is possibly the first single particle 3D reconstruction of frozen-hydrated HMM decorated actin at under 2 nm resolution. Our model suggests two distinct conformations for lever arm in the same biochemical state and provides a protocol for improving the resolution. The study is funded by the NIH/NIGMS.

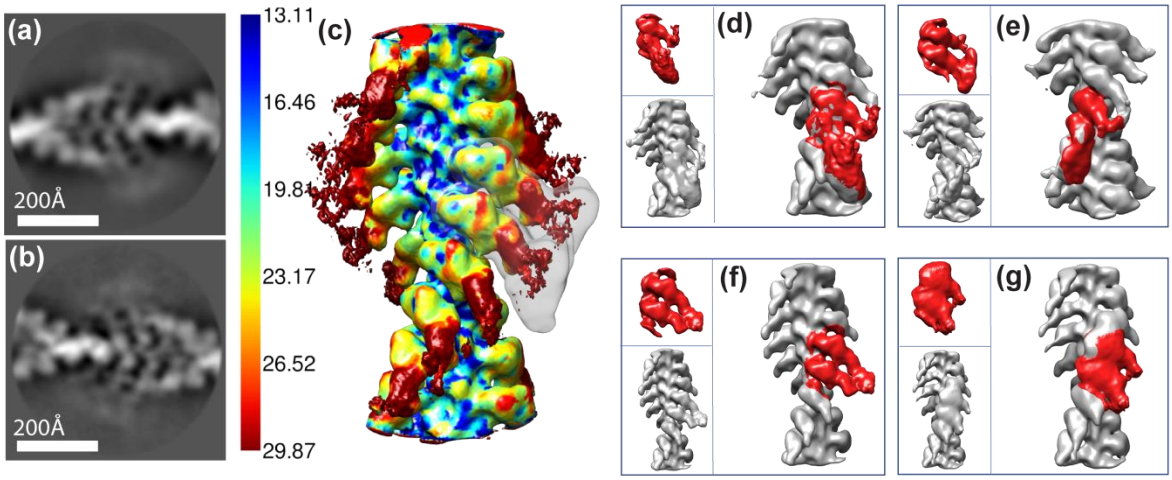

Figure 1. Figure 1. (a, b) 2D Class averages (Relion 3.1) showing the HMM decoration on actin (c) 3D density map showing parts of S1 domain with more details while lacking density corresponding to RLC domain, demonstrating the variation of the resolution. The translucent structure overlaying the region of the light chains shows the mask used for 3D classification (d-g) showing the result of 3D reconstruction

https://doi.org/10.1017/S1431927621003287 Published online by Cambridge University Press

of masked (shown as grey transparent density shown in (c)) 3D classification of the map shown in (c) including 2,697 segments in (d), 21,048 segments in (e), 17,394 segments in (f) and 9,070 segments in (g). Clarity of the region where the lever arms of the heads were best defined had little correlation with the number of class members.

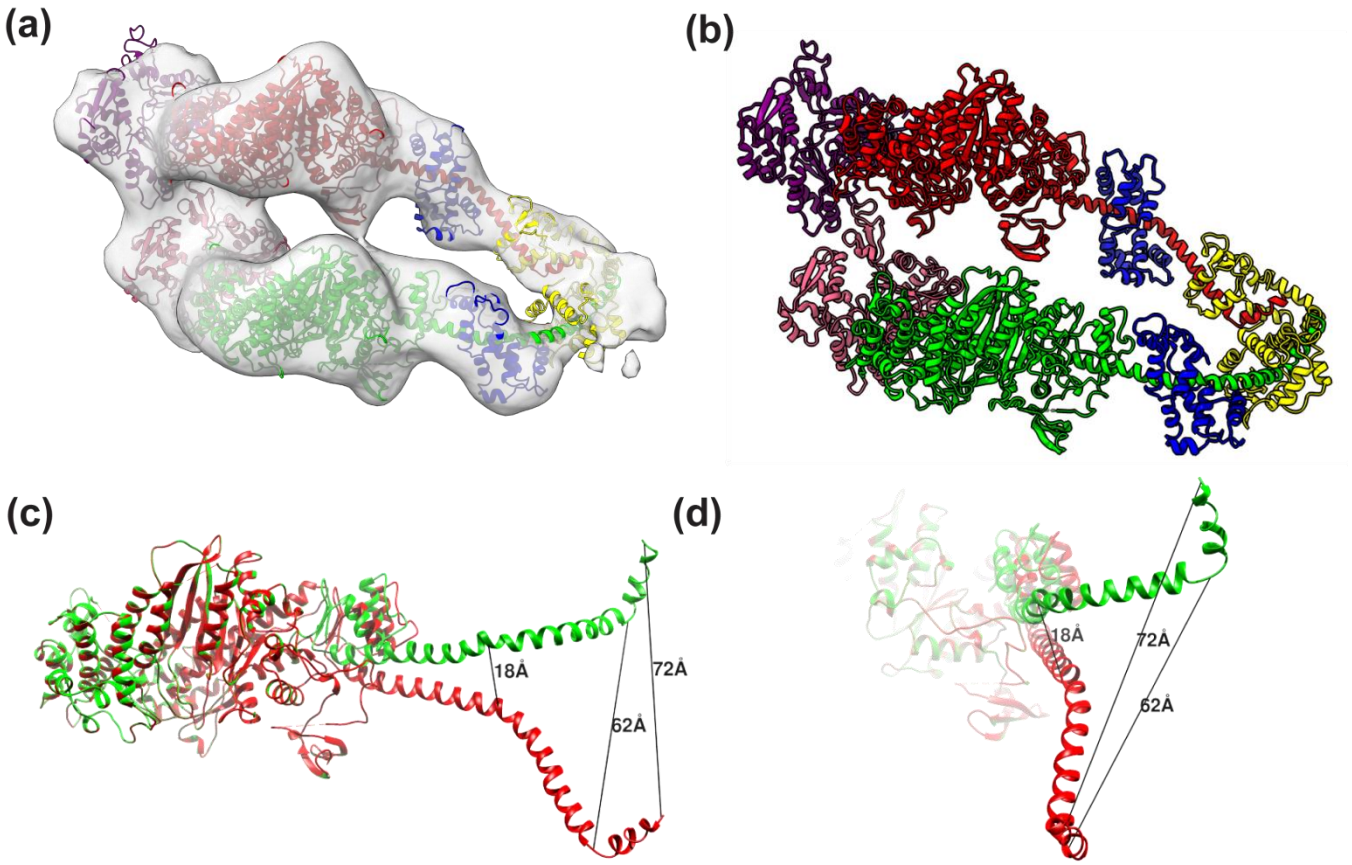

Figure 2. Figure 2. (a) showing the rigid body fitting of the atomic model (built as described) in segmented and then extracted map from Figure 1f. (b) showing the same atomic model with forward head (red), trailing head (green), ELCs (blue), RLCs (yellow) and actin subunits (pink and purple). (c, d) different views of the two heavy chains aligned using the motor domains. The filament axis is aligned with the y-axis of the page. This view shows the significant difference between the conformation of the two lever arms in the HMM, when bound to the thin filament using both heads in the same biochemical state.

References

1. M. A. Herzik, Jr., *Nature* **587**, 39-40 (2020).
2. S. Z. Chou, T. D. Pollard, *Proc Natl Acad Sci U S A* **116**, 4265-4274 (2019).
3. E. Behrmann *et al.*, *Cell* **150**, 327-338 (2012).
4. K. C. Holmes, M. A. Geeves, *Philos. Trans. R. Soc. Lond. B Biol. Sci.* **355**, 419-431 (2000).
5. J. Liu *et al.*, *J. Struct. Biol.* **147**, 268-282 (2004).
6. J. Liu *et al.*, *J Mol Biol* **362**, 844-860 (2006).
7. H. Kajiyama, *J Mol Biol* **204**, 639-652 (1988).
8. T. Wendt, D. Taylor, T. Messier, K. M. Trybus, K. A. Taylor, *J. Cell Biol.* **147**, 1385-1390. (1999).
9. D. W. Taylor, D. F. Kelly, A. Cheng, K. A. Taylor, *J Struct Biol* **160**, 305-312 (2007).
10. R. Danev, W. Baumeister, *Elife* **5**, (2016).

https://doi.org/10.1017/S1431927621003287 Published online by Cambridge University Press

11. T. Grant, A. Rohou, N. Grigorieff, *Elife* **7**, (2018).
12. S. He, S. H. W. Scheres, *J Struct Biol* **198**, 163-176 (2017).
13. J. L. Vilas *et al.*, *Structure* **26**, 337-344 e334 (2018).
14. C. Banerjee *et al.*, *J. Struct. Biol.* **200**, 325-333 (2017).
15. S. Yang *et al.*, *Nature* **588**, 521-525 (2020).
16. D. M. Himmel *et al.*, *Proc Natl Acad Sci U S A* **99**, 12645-12650 (2002).
17. A. Waterhouse *et al.*, *Nucleic Acids Res* **46**, W296-W303 (2018).
18. P. Emsley, K. Cowtan, *Acta Crystallogr D Biol Crystallogr* **60**, 2126-2132 (2004).

https://doi.org/10.1017/S1431927621003287 Published online by Cambridge University Press